Published in final edited form as:
NMR Biomed. 2013 April ; 26(4): 376–385. doi:10.1002/nbm.2871.

Dynamic Monitoring of Blood-Brain Barrier Integrity using Water Exchange Index (WEI) During Mannitol and CO_2 Challenges in Mouse Brain

Shuning Huang[1,2], **Christian T. Farrar**[2], **Guangping Dai**[2], **Seon Joo Kwon**[2], **Alexei A. Bogdanov Jr.**[3], **Bruce R. Rosen**[1,2], and **Young R. Kim**[2,§]

[1]Health Science and Technology (HST), Massachusetts Institute of Technology, Cambridge, MA 02139

[2]Athinoula A. Martinos Center for Biomedical Imaging, Massachusetts General Hospital, Charlestown, MA 02129

[3]University of Massachusetts Medical School at Worcester, MA USA

Abstract

The integrity of the blood-brain barrier (BBB) is critical to normal brain function. Traditional techniques for assessing BBB disruption rely heavily on the spatiotemporal analysis of extravasating contrast agents. But such methods based on the leakage of relatively large molecules are not suitable to detect subtle BBB impairment or to perform repeated measurements in a short time frame. Quantification of the water exchange rate constant (WER) across the BBB using strictly intravascular contrast agents could provide a much more sensitive method for quantifying the BBB integrity. For estimating the WER, we have recently devised a powerful new method using a water exchange index (WEI) biomarker and demonstrated BBB disruption in an acute stroke model. Here we confirm that the WEI is sensitive to even very subtle changes in the integrity of the BBB caused by (1) systemic hypercapnia and (2) low doses of a hyperosmolar solution. In addition, we have examined the sensitivity and accuracy of the WEI as a biomarker of the WER using computer simulation. In particular, the dependence of the WEI-WER relation on changes in vascular blood volume, T_1 relaxation of cellular magnetization, and transcytolemmal water exchange was explored. The simulated WEI was found to vary linearly with the WER for typically encountered exchange rate constants (1–4 Hz) regardless of the blood volume. However, for very high WER (>5 Hz) the WEI became progressively more insensitive to increasing WER. The incorporation of transcytolemmal water exchange, using a three-compartment tissue model, helped to extend the linear WEI regime to slightly higher WER, but had no significant effect for most physiologically important water exchange rate constants (WER<4 Hz). Variation in the

[§]**Corresponding author:** Young Ro Kim Assistant Professor, Harvard Medical School Harvard-MIT (HST) Athinoula A. Martinos Center for Biomedical Imaging Massachusetts General Hospital-East Bldg. 149, 13th Street Charlestown, MA 02129 Fax: 617-726-7422 spmn@nmr.mgh.harvard.edu.
Shuning Huang: shuning@nmr.mgh.harvard.edu
Christian T. Farrar cfarrar@nmr.mgh.harvard.edu
Guangping Dai: dai@nmr.mgh.harvard.edu
Alexei A. Bogdanov Jr.: Alexei.Bogdanov@umassmed.edu
Seon Joo Kwon: ksunj11@gmail.com
Bruce R. Rosen: bruce@nmr.mgh.harvard.edu

cellular T_1 had no effect on the WEI. Using both theoretical and experimental approaches, our study validates the utility of the WEI biomarker for monitoring BBB integrity.

INTRODUCTION

The integrity of the blood-brain barrier (BBB) is critical to normal brain function. In particular, the BBB plays a crucial role in maintaining the ionic homeostasis of the brain, delivering oxygen and nutrients to neuronal cells in the central nervous system (CNS), and protecting brain cells from neurotoxic or adversely neuroactive blood-borne agents. Alterations or breakdown in the BBB may initiate and/or contribute to pathological development and progression into irreversible brain damage. In ischemic and traumatic brain injury, opening of the BBB can lead to vasogenic edema, resulting in increased intracranial pressure, severe neurological damage, and even death. Damage to the BBB frequently accompanies the progression of numerous neurological disorders such as Alzheimer's disease, Parkinson's disease, and multiple sclerosis [1]. Therefore, the development of methods to study pathological changes of the BBB would help greatly to better understand the disease progression, thereby aiding the development of effective treatment options, and to assess the efficacy of pharmacological interventions.

Despite the great need, strategies to accurately evaluate the BBB functionality have not been successful, particularly for quantifying subtle changes in the BBB integrity. The most commonly used methods for assessing BBB disruption are based on studying the spatiotemporal extravasation of exogenous markers such as staining dyes [2,3], fluorescein [4], radiolabeled compounds [5–7], and gadolinium-based MRI contrast agents [8]. However, extravasation of these markers is dependent on the extent and severity of the BBB damage as well as the biophysical properties, such as size and charge, of the markers themselves. Therefore, these methods are only useful when the BBB is compromised to the extent that the disruption allows extravasation of these relatively large molecular weight markers (>500 Da) and are not sensitive to subtle and early changes in the BBB permeability. In addition, *ex vivo* methods generally require sacrifice of the animal and destruction of the brain tissue at a specific time point of interest, thus precluding longitudinal monitoring. Similarly, current *in vivo* MRI methods require a complete systemic clearance of contrast agent for repeated vascular permeability measurements and are thus not repeatable on a time frame shorter than the clearance time of the molecular weight markers (typically many hours). For understanding the mechanisms of rapid changes in the BBB, such as the progressive BBB deterioration in acute ischemic stroke, it is necessary to quantify dynamic changes that occur during BBB disruption before the leakage of such large contrast agents is apparent. Therefore, the development of a method that enables the detection of early, subtle changes in the integrity of the BBB and permits repeated quantitative monitoring of BBB alterations is highly desirable.

Previously, Donahue et al. [9] showed that the measurement accuracy of the absolute cerebral blood volume (CBV) using intravascular MRI contrast agents could be significantly affected by the rate of water exchange across the BBB due to the sensitivity of the MRI signal to water exchange between the vascular and interstitial spaces. Based on this

observation, we previously presented a novel MRI method to characterize the BBB integrity by utilizing the dependence of the spoiled gradient-echo MR signal intensity on vascular-interstitial water exchange to calculate a water exchange index (WEI), defined as the ratio between the *apparent* CBV calculated from the spoiled gradient-echo MR signal intensity measured using a relatively small flip angle (an exchange-sensitive regime) and the *absolute* CBV calculated from the signal intensity measured using a relatively large flip angle (an exchange-insensitive regime) [10]. This MRI technique does not require accurate tissue or blood T_1 measurements or model fitting, unlike the method previously proposed by Schwarzbauer et al. [11]. Therefore, utilizing only the MRI signal intensity, our technique can be easily implemented without the need for sophisticated multi-parameter fitting algorithms or model-based estimations.

We previously demonstrated the utility of this method to investigate the overall BBB integrity in animal models of brain tumors and ischemic stroke [10,12,13]. However, the BBB disruption caused in the stroke and tumor models was quite significant. For experimentally demonstrating the feasibility of quantitatively monitoring subtle alterations in the BBB integrity, we propose to dynamically and quantitatively monitor the effects of both graded systemic hypercapnia and repeated administrations of a hyperosmolar solution of Mannitol on the WEI and the CBV. Although the phenomena we are interested in here have been observed previously, no detailed documentation is available for quantifying specific changes in cerebrovascular water permeability during either CO_2 or Mannitol challenges. We posit that quantifying the magnitude of the induced cerebrovascular changes to graded BBB perturbations will be highly useful for understanding cerebrovascular reactivity and associated pathological status of the BBB.

In our previous studies, simulations of the WEI dependence on the water exchange rate constant were performed using a two-compartment tissue model (vascular and extravascular/extracellular compartments), where the water exchange rate constant across the cellular membrane is assumed to be zero and therefore the cellular space does not need to be considered. However, both water exchange across the cell membrane (i.e. transcytolemmal water exchange) and cellular volume fraction have been shown to affect the actual experiment and the data interpretation [10,14–16]. Although a recent study has reported the transcytolemmal water exchange rate constant to be an order of magnitude slower than that across the erythrocyte membrane [17], literature values of the estimated transcytolemmal water exchange rate constant varies from as low as 0.25 to 20 Hz [10], thus challenging the current two-compartment model. Additionally, despite the different biological compositions of the interstitial and cellular spaces, previous studies were based on a simple two-compartment model that assumed a single T_1 value for both the intra- and extra-vascular/extra-cellular compartments. To explore the influence of the transcytolemmal water exchange rate constant and cellular volume fraction on the CBV and WEI measurements we therefore incorporated the cellular space into the previously described two-compartment water exchange model. In particular, the dependence of the WEI on a wide range of T_1 differences between cellular and interstitial magnetization, transcytolemmal water exchange rate constant, and varying cellular volume were explored.

The current studies were thus undertaken to (1) investigate the sensitivity of the WEI technique for measuring dynamic changes in CBV and water exchange across the BBB during subtle perturbations of the cerebrovascular physiology, and (2) to understand the effects of the cellular space and transcytolemmal water exchange on the quantification and sensitivity of the CBV and WEI.

MATERIALS AND METHODS

The three-compartment water exchange model

A previously described two-compartment water exchange model [10] was extended by further dividing the extravascular space into an extravascular/extracellular space (i.e., interstitial space) and a cellular space (Figure 1), similar to that described by Li et al [18]. In this three-compartment water exchange model, it is assumed that there is no direct water exchange between the vascular and cellular spaces. The modified Bloch equations [19] after incorporating the water exchange phenomena [20,21] can be described as:

(1)

(2)

(3)

where $M_b(t)$, $M_i(t)$, and $M_c(t)$ are the time-dependent magnetizations in the vascular (blood), interstitial, and cellular spaces, respectively. $T_{1,b}$, $T_{1,i}$, and $T_{1,c}$ are the longitudinal relaxation time constants of the magnetization in the vascular, interstitial, and cellular compartments, respectively. $k_{b,i}$ and $k_{i,b}$ are the rate constants for water exchange from the vascular space to the interstitial space, and from the interstitial space back to the vascular space, respectively. Parameters $k_{i,c}$ and $k_{c,i}$ are the rate constants for water exchange from the interstitial space to the cellular space and from the cellular space back to the interstitial space, respectively. At any particular moment, the total magnetization is equal to the sum of the magnetizations from the three-compartments:

(4)

Furthermore, under the condition of mass balance, at equilibrium:

(5)

(6)

The water exchange rate constant (WER) is finally given by:

 (7)

where PS is the permeability surface area and V is the blood volume.

Computer simulation

The 3D spoiled gradient-echo signal intensity of the brain tissue was simulated using the three-compartment model described above. Tissue signal was obtained by solving the coupled Bloch equations (Equation 1, 2, and 3) numerically for different water exchange rate constants (ranging from 1 Hz up to 16 Hz across the BBB or cell membrane), compartment volumes (vascular volume ranging from 1% to 10% of the total volume, the ratio of interstitial volume to cellular volume of 1:4), and pulse sequence parameters (i.e., flip angle α with a fixed TR of 30 ms). All simulations were performed for a magnetic field strength of 9.4 Tesla with a blood T_1 of 2.3 sec, interstitial T_1 of 1.8 sec, and cellular T_1 ranging from 1.5 to 2.1 sec. The magnetizations (M_b, M_i, and M_c) following each RF excitation were calculated by solving the coupled Bloch equations (Equation 1, 2, and 3) until a steady state was reached. The MRI signal intensity (SI) was then obtained from the sum of the steady-state magnetizations (M^{ss}) of the three compartments using Equation 8. Next the *apparent* blood volume (CBV^{app}) was calculated at different flip angles, assuming no water exchange between compartment spaces, from the difference in MRI signal intensity measured pre- and post-injection of Gd-PGC as given by Equation 9. The WEI was obtained by taking the ratio of the CBV^{app} at 20° to that at 90° (Equation 10).

 (8)

 (9)

 (10)

Intra-vascular MR imaging contrast agent

Protected graft copolymers bearing covalently linked Gd-DTPA residues (Gd-PGC) were synthesized and purified as described previously [22]. The batches of Gd-PGC were characterized on size-exclusion HPLC columns (TSK3000SW, Supelco, Bellefonte PA) and gadolinium concentrations were determined by elemental analysis. The polymer was dissolved at 50 mg/ml (13 mM Gd) in DPBS, at pH 7, and sterile-filtered.

Animal preparation

All experiments were conducted in accordance with the guidelines and regulations of the Subcommittee on Research Animal Care of Massachusetts General Hospital. A total of 13 male C57BL/6 mice (10 – 12 wks old, and about 20g each) were used in this study. Seven of the mice were prepared with a femoral vein cannula in each hind leg; one for constant Mannitol infusion and the other for contrast agent and Mannitol bolus injection. The other six mice were used for the CO_2 challenge.

Continuous inhalation of gas mixture (30% O_2 and 70% N_2O) with 1.5% isoflurane was used for anesthesia during the surgical preparations. Immediately following the surgery, mice were relocated to a stereotaxic frame designed for MRI acquisition. During the MRI acquisitions, the mice were anesthetized with 1.5% isoflurane in a 1:1 gas mixture of medical air (78% N_2 and 21% O_2) and oxygen while body temperature was monitored and maintained at ~36.5°C.

MRI acquisition

All MRI experiments were performed at 9.4T (Bruker Biospin, Billerica, MA) with a gradient coil (Resonance Research, Billerica, MA) capable of generating a 150 Gauss/cm field gradient. A volume head coil, specifically designed for mouse head imaging, was used for all image acquisitions. To eliminate the in-flow effect in 2D acquisition, we used a 3D SPGR (spoiled gradient-echo) pulse sequence. 3D images were acquired with TR/TE = 30/3 ms, matrix size = 64 × 64 × 128, FOV = 1.6 × 1.6 × 3.2 cm, number of averages = 1, and varying flip angles of 20°, 30°, 60°, and 90°. Additionally, the 3D SPGR scan was performed with TR/TE = 30/[5.0, 7.0] ms at the fixed flip angle of 30°. The multi-echo data were used to calculate regional T_2* relaxation time constants as described below in the data analysis. Prior to and following contrast agent administration (Gd-PGC: 17 μmol Gd/kg), two sets of 3D images were acquired for baseline CBV and WEI measurements, respectively.

For the Mannitol group (n=7), baseline data was acquired using a 3D SPGR with varying flip angles and gradient-echo times. Following baseline image acquisition three Mannitol boluses (100 μl of 20% Mannitol solution delivered over 20 sec) were delivered every 30 minutes. Between each bolus injection, a 20% Mannitol solution was continuously infused at a rate of 100 μl/hr to maintain the systemic blood concentration of Mannitol. Two sets of 3D volumetric images, as described above, were acquired immediately and 15 minutes after each bolus injection.

For the animal group that underwent the CO_2 challenge (n=6), we used four different CO_2 doses (2.5%, 5.0%, 7.5%, and 10.0%). Graded hypercapnia experiments were performed after acquisition of baseline (i.e. 50% O_2 and 50% medical air) data, using the same 3D SPGR sequence with varying flip angles and gradient-echo times. For each CO_2 level, the MR images were collected after each animal was given the specified CO_2 gas for 5 minutes.

Data analysis

We used region of interest (ROI) analysis to investigate changes of absolute cerebral blood volume (CBV) and WEI under different physiological conditions, i.e., baseline, Mannitol injection, and CO_2 challenge. The ROI pertaining to the blood compartment was drawn within the inferior cerebral vein (http://www.informatics.jax.org/). To minimize partial volume effects, only blood pools at least three voxels in width and more than three slices in length were used for selection of the venous blood ROI. The area of cerebral cortex supplied by the middle cerebral artery (MCA) was manually outlined based on the Paxon mouse brain atlas [23]. We calculated the CBV using Equation 9, based on images acquired using a 90° flip angle, and evaluated the WEI with Equation 10. Since the intravascular contrast agent can also affect transverse (T_2 or T_2*) relaxation, we calculated the regional T_2* from mono-exponential fits of the 3D SPGR signal intensity as a function of TE (i.e., 3.0, 5.0, and 7.0 ms). The T_2*value was used to obtain a purely T_1-weighted signal intensity, required for accurate CBV and WEI estimations. While independent T_2* values may exist for each compartment, the use of a mono-exponential fit greatly simplifies the data analysis and we have found the CBV and WEI values obtained to be in good agreement with those determined from an ultra-short echo time (UTE) sequence with a TE of 0.025 ms, suggesting that the mono-exponential T_2* assumption is valid for the measurement of CBV and WEI. In addition, the physical extent of the susceptibility gradient induced by the intravascular Gd-PGC is much greater than the size of the interstitial and cellular micro compartments and it is therefore reasonable to expect to observe a single average T_2* rate constant. In contrast, the intravascular Gd-PGC has minimal direct influence on the T_1 of the interstitial and cellular magnetizations and the dependence of the WEI on a range of interstitial and cellular T_1's was therefore explored in simulations as discussed above.

WER calculations

To validate the relation between the experimental WEI and the WER derived from the tissue compartment model, we fit the flip-angle dependence of the experimentally determined CBV values to extract the WER for cortex ROIs from all 13 animals (58 total experimental conditions: 7 mice with 4 Mannitol levels and 6 mice with 5 CO_2 levels). The fitting algorithm used the two-compartment model and the experimental parameters (i.e. TR and flip-angles) and experimentally measured T_1's (brain tissue and blood) before and after contrast agent injection. The two-compartment model was used as the fitting is greatly simplified and there was no significant difference between the two- and three-compartment models over the range of most water exchange rate constants observed experimentally (1–4 Hz), irrespective of blood volume. The experimental WEI was then plotted as a function of the fitted WER for all data sets in which the flip angle dependence of the measured CBV was physically reasonable (i.e., CBV quantified at a smaller flip angle is always greater than CBV quantified at a larger flip angle: n = 11).

Statistical test

Unless otherwise specified, we performed all statistical analyses for the ROI presented in the study using a two-tailed paired t-test. For correlation analysis, we applied the Pearson product-moment correlation test (and linear regression). Data were presented as average ±

standard error of the mean. Statistical significance was accepted at a confidence level of 0.95.

RESULTS

WEI Simulations

Figure 2A demonstrates the effects of intravascular blood volume (i.e., CBV) and vascularinterstitial WER on the WEI calculation with and without transcytolemmal water exchange. An increase in the vascular volume fraction leads to a decrease in the WEI, even as the WER remains unchanged. With increasing vascular volume, the actual WER values are underestimated as the non-linearity between the WEI and the WER intensifies (note that the two-compartment vascular/extravascular volume fractions of 0.01 and 0.05 translate to vascular/interstitial volume ratios of 0.0526 and 0.333 when including the cellular volume in the three-compartment model). The effect of such changes in vascular volume fraction on the WEI becomes pronounced only when the actual WER becomes significantly higher (>2Hz) than that of the intact BBB (~1Hz). This effect could change the measured WEI by as much as ~20% when the transvascular WER is 6 Hz even within the physiologically relevant range of vascular volume (between 0.01 and 0.05). The inclusion of the transcytolemmal water exchange has almost no effect on the WEI-WER relation for water exchange rate constants less than 3 Hz, irrespective of blood volume. However, transcytolemmal water exchange does slightly improve the linearity of the WEI-WER relation for high water exchange rate constants (>4 Hz) and blood volumes (5%). Finally, Figure 2B shows that the dependence of the WEI on the T_1 of cellular magnetization is negligible for two vascular volume fractions (i.e., 0.02 and 0.04).

Animal experiments

Representative T_1-weighted images from four different brain regions pre and post contrast agent injection are shown in Figure 3A. Figure 3B is an MRI angiogram of a typical mouse brain, acquired with a 3D gradient-echo sequence. T_1-weighted signals from large blood vessels and venous sinuses are clearly visible after intravenous Gd-PGC injection. No evidence of contrast agent leakage into the tissue is observed as demonstrated in Figure 4. Simulations of the normalized tissue signal intensity pre and post Gd-PGC for various CBVs demonstrate only a slight signal increase following contrast agent injection due to the increased signal in the vascular space (Figure 4A). Contrast agent extravasation into the brain tissue, which is not modeled in the simulations, would lead to a significantly greater increase in the tissue signal intensity post Gd-PGC. Therefore, the experimentally observed small increase in cortex tissue signal intensity for both Mannitol and CO_2 challenges following Gd-PGC injection (Figure 4B), similar to that observed in the simulations, is consistent with no contrast agent extravasation into the tissue. As shown in Figure 4C, MRI signal in the blood post-contrast remained time-independent, indicating a long blood half-life of Gd-PGC in the mouse. The baseline CBV in the mouse cerebral cortex was 2.59% ± 0.18%, and the WEI was 1.49 ± 0.07.

Temporal changes in the fractional cerebral blood volume (CBV) and the water exchange index (WEI) induced by serial injections of Mannitol boluses are shown in Figure 5. The

CBV and WEI were calculated using Equations 9 and 10, respectively. Both CBV and WEI in the cerebral cortex increased significantly following the initial intravenous Mannitol injection. CBV continued to increase with subsequent Mannitol injections, with statistically significant CBV changes observed over each Mannitol bolus (Figure 5A). On average, the WEI was also higher after the second and the third bolus injections than after the first bolus. However, unlike the CBV, no statistically significant increase was attained for the WEI, indicating that the Mannitol-induced BBB opening is maximized after the first bolus. The WEI remained statistically higher than baseline WEI throughout the experiment (Figure 5B).

The responses of the CBV and WEI to CO_2 challenge are shown in Figures 6A and 6B, respectively. The CBV increased significantly after each increase of CO_2 level in the breathing gas mixture (Figure 6A). In addition, the increase of CBV is linearly proportional to the percent CO_2 in the gas mixture. The response of the CBV plateaued when the amount of CO_2 was increased from 7.5% to 10%. The WEI, on the other hand, showed a different trend. The WEI was significantly higher than the baseline value for each CO_2 challenge. However, no statistical difference in WEI was observed when the amount of CO_2 was increased from 2.5% to 5%, 7.5%, and 10%, respectively (Figure 6B). Both CBV and WEI drastically decreased to near the baseline values after we switched the breathing gas mixture from 10% CO_2 to 100% O_2 (Figure 6A and 6B).

Theoretically, both the size of the cellular compartment and the transcytolemmal water exchange rate constant could have significant effects on the WEI calculation (Figure 2A and 2B). In order to demonstrate the practical range and possible errors associated with the proposed WEI method, we calculated the vascular-interstitial water exchange rate constant (WER) using multi-parametric fitting of the flip-angle dependence of the experimental CBV measurements based on the two-compartment tissue model and compared the results with the experimentally measured WEI. The two-compartment model was employed instead of the three-compartment model since no significant differences were observed between models in simulations (Figure 2) performed over most of the range of water exchange rate constants observed experimentally (1–4 Hz). The scatter plot of the WEI as a function of the WER (Figure 7) showed that the experimental WEI was linearly related to the calculated WER, indicating the degree of BBB water exchange can be accurately assessed using the WEI in the physiologically important water exchange range (i.e., <4Hz). A slight non-linearity in the experimentally measured WEI-WER relation was expected for WER >4 Hz based on the simulation results (see Figure 2) and was observed in the experimental WEI-WER scatter plot (Figure 7).

DISCUSSION

In order to model subtle alterations in the blood-brain barrier integrity (BBB), we employed systemic hypercapnia and low doses of a hyperosmolar solution of Mannitol. The use of hypercapnia and mannitol are well-established physiological and pharmacological challenges known to change both cerebral blood volume (CBV) and blood-brain barrier (BBB) permeability.

WEI and CBV response to Mannitol

Mannitol, an osmotic agent, has been widely used clinically to reduce edema and acutely raised intracranial pressure, as well as to open the BBB for drug delivery to the CNS [24,25]. Administration of Mannitol can both generate an osmotic pressure gradient across the BBB and cause shrinkage of endothelial cells, causing the BBB to open and the CBV to increase [26]. For the normal healthy BBB, previous studies have shown that opening of the BBB is dependent on both the infusion time and the concentration of the osmatic agent [26]. Long infusion time or high concentration alone has little effect on the BBB permeability unless a particular threshold of combined infusion time and concentration is reached [26]. To induce transvascular opening of the BBB for exogenous agents, such as Evans Blue, most animal model studies have required Mannitol concentrations of at least 1.4 M to 1.6 M [26]. This range of Mannitol concentration is 20–30% higher than the one used in this study (1.1 M). Therefore, the osmolarity change caused by the initial injection of Mannitol in our study was likely insufficient to achieve effective BBB opening for large molecules to extravasate. The significant increase observed in the WEI as a result of the low dose Mannitol injection supports the hypothesis that using water as a biomarker provides a more sensitive and direct measure for assessing BBB integrity and detecting damage than quantifying vascular permeability based on the extravasation of relatively large exogenous contrast agents.

However, a significant increase in WEI was observed after only the first Mannitol bolus injection (Figure 5A); the measured WEI values remained constant at approximately the same level after subsequent bolus injections and prolonged infusion (100 μl/hr) of relatively low concentration Mannitol (1.1 M). Although there was a trend of increased WEI after repeated Mannitol administrations, these additional increases in WEI did not reach statistical significance when compared to the WEI measured immediately after the first Mannitol bolus (Figure 5B). This finding suggests that hyperosmolar disruption of the BBB may already be maximized for water molecules with the initial Mannitol injection dose. In contrast to the WEI, the CBV continued to increase significantly after each additional Mannitol injection (Figure 5A), which is likely due to the difference in osmotic pressure across the BBB. Such increases in CBV after repeated Mannitol administration are in agreement with the previous PET [27] and MRI [28] studies.

WEI and CBV response to CO_2

Elevation of the partial pressure of arterial CO_2 (pCO_2) has a strong vasodilatory effect, leading to an increase in CBV that is dependent on the level of arterial pCO_2 [29,30]. Moreover, hypercapnia (i.e., increased pCO_2) has been shown to cause an increase in BBB permeability in experimental animals [31–33]. In the current study, we found that the CBV increase varied approximately linearly with the amount of CO_2 in the breathing gas mixture (Figure 6A), which agrees in general with published literature results [30]. The CBV increase reached a plateau only at 10% CO_2. We also observed a significant increase in the WEI during the graded hypercapnia exposure. As suggested by the studies of Johansson, et al. [34] and Mollgard and Sorensen [2], this observed increase in BBB water exchange is closely linked to the increase in vascular permeability that is associated with hypercapnia-induced vasodilation. Such increases in water exchange rate were reversible; with exposure

to 100% O_2, not only did the CBV return to the baseline, so too did the WEI (Figure 6B). We also note that the WEI increased significantly during 2.5% CO_2 inhalation and stayed at the approximately same level throughout the graded hypercapnic episodes involving higher CO_2 levels. This trend is very similar to that observed during serial Mannitol injections.

The initial vascular volume increase and concomitant increase in the transvascular WER indicate that CO_2-induced vasodilation may be a potent factor in the increased BBB permeability observed. One possible mechanism responsible for this phenomenon is the disjointing of endothelial tight junctions. Since the vessel wall tension is proportional to the pressure and vessel radius and inversely proportional to vessel wall thickness, dilated vessels experience higher tension at a given intraluminal pressure, leading to increased endothelial tight junction permeability. The fact that the WEI remained at a constant value despite the further increase in CBV for both CO_2 and Mannitol challenges suggests that increased vessel dilation beyond a certain point has no further effect on the WEI. On the other hand, since the observed increases in WEI were not proportional to graded CO_2 levels, we cannot preclude the possibility that CO_2-induced changes in the WEI are triggered by on/off responses of water channels such as aquaporins [35]. Similar observations were previously made in hyper-acute stages of stroke progression, where the initially increased transvascular water exchange rate constant immediately after stroke was sustained at a constant level despite the progressive ischemic damage to the brain tissue [10]. As mentioned above, the measured WEI and CBV were reversible and returned to near the baseline upon the change of gas from 10% CO_2 (with 45/45% medical air/ O_2) to 100% O_2. Such findings reveal that water exchange across the BBB may be actively regulated for maintaining minimal transport of water through the vascular wall.

Comparison of BBB perturbations: CO_2, Mannitol, tumor, stroke

The increased WEI observed with 2.5% CO_2 indicates that vessel dilation alone is sufficient to cause elevated WEI and BBB permeability, as previously suggested by Rapoport et al. [26,36]. Three injections and continuous infusion of Mannitol resulted in overall increases in the CBV and WEI of 0.038 ± 0.0027 and 1.87 ± 0.13, respectively. These results are nearly identical to the CBV and WEI values measured using 2.5% CO_2. This suggests that vasodilation associated with increased CBV, independent of hyperosmolar effects, could account for a large fraction of the observed WEI increase observed with low dose Mannitol administration. On the other hand, it is noteworthy that the fluid sources of vasodilation for the CO_2 and Mannitol challenges are different. For hypercapnia, the apparent vasodilation is mostly due to the blood volume increase from the increased blood flow. For the Mannitol challenge, the source is the stromal water as demonstrated by its ability to reduce edema and the associated intracranial pressure. Despite this difference, increased water movement across the BBB was detected for both challenges.

While vasodilation appears to play a critical role in the elevated WEI for CO_2 and Mannitol challenges, there are many other mechanisms that can lead to elevated WEI and BBB permeability. For example, while the CBV is dramatically elevated in solid brain tumors, the increased CBV is not due to vessel dilation. Indeed, previous studies have demonstrated that brain tumor vascular reactivity is significantly reduced [37]. Instead, the increased vascular

permeability of the BBB is attributed to abnormal vessel growth induced by up regulation of vascular endothelial growth factors (VEGF), angiopoietin-2 (ANG2), and other vascular growth factors. VEGF promotes the growth of new, immature blood vessels, while ANG2 destabilizes vascular structures to promote vascular remodeling. The net result is an increase in vessel density, average vessel diameter, and vascular permeability. Despite the different mechanism of BBB disruption, we previously found the WEI to be sensitive to subtle, early changes induced in BBB permeability by tumor cells that are not detectable using extravasation of Gd-DTPA [38]. In addition, we previously reported that the WEI increased as the CBV *decreased* in acute stages of permanent ischemia [10]. Clearly neither vasodilation nor angiogenesis play a role in the disrupted BBB in stroke. Instead, a number of recent studies suggest that up-regulation of aquaporin-4 (AQP4) may play an important role in the vasogenic edema associated with stroke [39].

As demonstrated by the above studies, the WEI is very sensitive to a wide range of BBB perturbations. In addition, the fact that elevated WEI have been observed over a wide range of cerebral blood volumes, from low (stroke) to high (tumor, CO_2, Mannitol), suggests that the WEI can be measured regardless of variations in CBV.

Sensitivity of the WEI biomarker to changes in the WER

We initially designed the WEI method to provide a simple, efficient and repeatable method for the longitudinal quantification of the transvascular water exchange rate constant (WER). However, previous simulations based on the two-compartment tissue model revealed that the WEI might be dependent on biophysical factors other than the actual vascular-interstitial WER, such as the CBV and interstitial volume. As previously discussed, such deviations suggest that the WEI may not be sensitive to the WER under extreme physiologic conditions (i.e., large WER and blood volume) where the linearity of the WEI-WER relation breaks down. Computer simulations using the two-compartment tissue model revealed that, for very high exchange across the vascular membrane (WER>5 Hz), the WEI does underestimate the WER (Figure 2). Increasing blood volume exacerbated this non-linearity or insensitivity of the WEI to changes in the WER at high WERs. In contrast, the addition of transcytolemmal exchange to the three-compartment model showed a slight reduction in such relative underestimations of the WER by the WEI in the high exchange regime (Figure 2B). However, for relatively low water exchange rate constants (1–4 Hz), there is no significant difference between two- and three-compartment model simulations and the WER is linearly correlated with the WEI. The simulation results below 4 Hz are in good agreement with the experimental results where the experimentally measured WEI is linearly correlated with the WER determined from two-compartment exchange model fitting of the flip-angle dependence of the CBV^{app} (Figure 7). Therefore, both computer simulation and animal experiment confirmed that the WEI is linearly proportional to the WER in the physiologically important range of 1–4 Hz and can be used to evaluate the change of the WER across the BBB. For higher water exchange rate constants (> 4Hz) the experimental WEI-WER relation deviated slightly from linearity in agreement with the behavior observed in the simulations (Figure 2). While successful fitting of the flip-angle dependence of the CBV to obtain an absolute WER was possible, it does require the acquisition of multiple T1-weighted images with different flip angles as well as accurate T1 maps. In addition, the

complex multi-parameter fitting likely introduces additional uncertainty in the WER, which is only exacerbated for the three-compartment model with additional fitting parameters. This highlights the advantage of the WEI, which is not dependent on complex multi-parameter model fitting and does not require additional, time-consuming data acquisition. Finally, since the WER is related to the BBB water permeability (see Equation 7) we can also estimate the change in BBB water permeability by simultaneously measuring the WEI and absolute CBV.

Summary

Water molecules are ideal biomarkers for probing the BBB integrity since they are naturally abundant and permeable through the intact BBB. We have shown that the WEI is sensitive to even subtle changes in transvascular water exchange induced by graded hypercapnia and Mannitol challenges to the BBB integrity. These BBB perturbations have previously been shown to be insufficient for detecting extravasation of exogenous markers, indicating that the WEI is a more sensitive biomarker of BBB integrity. Furthermore, we validated the use of the WEI as a biomarker of transvascular water exchange by revealing a strong linear correlation between the experimental WEI and the WER determined from fitting the flip-angle dependence of the experimental CBV measurements. In addition, computer simulations of the WEI using a three-compartment tissue model demonstrated that the inclusion of transcytolemmal water exchange had no effect on the WEI-WER relation for most physiologically relevant water exchange rate constants (<4 Hz), irrespective of blood volume. The transcytolemmal water exchange did slightly increase the accuracy of the WEI measurements under extreme vascular conditions with high WER (>4 Hz) and blood volume fraction (0.05). Since many diseases affecting the central nervous system are associated with damage or disruption of the BBB, this novel WEI technique provides a convenient means to simultaneously monitor alterations in BBB integrity as well as possible changes in CBV. These novel biomarkers may help improve our understanding of the pathophysiological mechanisms of BBB disruption associated with disease progression, promote the discovery of therapeutic treatment options, and provide a biomarker for the assessment of the efficacy of such treatments.

Acknowledgments

This work is supported by the NIH grant 5R01EB002066-17, the American Heart Association SDG #0835451N, and NIH grant S10RR025563.

Funding support: NIH grant 5R01EB002066-17 and the American Heart Association SDG #0835451N

Abbreviations

BBB	(blood-brain barrier)
WER	(water exchange rate constant)
WEI	(water exchange index)
CNS	(central nervous system)
CBV	(cerebral blood volume)

Gd-PGC (Gadolinium protected graft copolymers)

SPGR (spoiled gradient-echo)

UTE (ultra-short TE).

REFERENCES

1. Zlokovic B. The blood-brain barrier in health and chronic neurodegenerative disorders. Neuron. 2008
2. Mollgard, KSS. The Pathology of Cerebral Microcirculation. De Gruyter and Co.; Berlin: 1974. The permeability of cerebral capillaries to a tracer molecule, Alcian blue, with a molecular weight of 1390.
3. Suzuki R, Yamaguchi T, Kirino T, Orzi F, Klatzo I. The effects of 5-minute ischemia in Mongolian gerbils: I. Blood-brain barrier, cerebral blood flow, and local cerebral glucose utilization changes. Acta Neuropathologica. 1983; 60(3–4):207–216. [PubMed: 6613530]
4. Belayev L, Busto R, Zhao W, Ginsberg MD. Quantitative evaluation of blood-brain barrier permeability following middle cerebral artery occlusion in rats. Brain research. 1996; 739(1–2):88–96. [PubMed: 8955928]
5. Chi OZ, Wei HM, Lu X, Weiss HR. Increased blood-brain permeability with hyperosmolar mannitol increases cerebral O2 consumption and O2 supply/consumption heterogeneity. J Cereb Blood Flow Metab. 1996; 16(2):327–333. [PubMed: 8594066]
6. Preston E, Foster DO. Evidence for pore-like opening of the blood-brain barrier following forebrain ischemia in rats. Brain research. 1997; 761(1):4–10. [PubMed: 9247060]
7. Gotoh O, Asano T, Koide T, Takakura K. Ischemic brain edema following occlusion of the middle cerebral artery in the rat. I: The time courses of the brain water, sodium and potassium contents and blood-brain barrier permeability to 125I-albumin. Stroke. 1985; 16(1):101–109. [PubMed: 3966252]
8. Jiang Q, Ewing JR, Ding GL, Zhang L, Zhang ZG, Li L, Whitton P, Lu M, Hu J, Li QJ, Knight RA, Chopp M. Quantitative evaluation of BBB permeability after embolic stroke in rat using MRI. J Cereb Blood Flow Metab. 2005; 25(5):583–592. [PubMed: 15716859]
9. Donahue KM, Weisskoff RM, Chesler DA, Kwong KK, Bogdanov AA Jr. Mandeville JB, Rosen BR. Improving MR quantification of regional blood volume with intravascular T1 contrast agents: accuracy, precision, and water exchange. Magnetic Resonance in Medicine. 1996; 36(6):858–867. [PubMed: 8946351]
10. Kim YR, Tejima E, Huang S, Atochin DN, Dai G, Lo EH, Huang PL, Bogdanov A Jr. Rosen BR. In vivo quantification of transvascular water exchange during the acute phase of permanent stroke. Magnetic Resonance in Medicine. 2008; 60(4):813–821. [PubMed: 18816832]
11. Schwarzbauer C, Morrissey SP, Deichmann R, Hillenbrand C, Syha J, Adolf H, Noth U, Haase A. Quantitative magnetic resonance imaging of capillary water permeability and regional blood volume with an intravascular MR contrast agent. Magnetic Resonance in Medicine. 1997; 37(5): 769–777. [PubMed: 9126952]
12. Kim YR, Rebro KJ, Schmainda KM. Water exchange and inflow affect the accuracy of T1-GRE blood volume measurements: implications for the evaluation of tumor angiogenesis. Magnetic Resonance in Medicine. 2002; 47(6):1110–1120. [PubMed: 12111957]
13. Kim YR, Savellano MD, Savellano DH, Weissleder R, Bogdanov A Jr. Measurement of tumor interstitial volume fraction: method and implication for drug delivery. Magnetic Resonance in Medicine. 2004; 52(3):485–494. [PubMed: 15334566]
14. Zhou R, Pickup S, Yankeelov TE, Springer CS Jr. Glickson JD. Simultaneous measurement of arterial input function and tumor pharmacokinetics in mice by dynamic contrast enhanced imaging: effects of transcytolemmal water exchange. Magnetic resonance in medicine : official journal of the Society of Magnetic Resonance in Medicine / Society of Magnetic Resonance in Medicine. 2004; 52(2):248–257.

15. Donahue KM, Weisskoff RM, Burstein D. Water diffusion and exchange as they influence contrast enhancement. J Magn Reson Imaging. 1997; 7(1):102–110. [PubMed: 9039599]
16. Landis CS, Li X, Telang FW, Molina PE, Palyka I, Vetek G, Springer CS Jr. Equilibrium transcytolemmal water-exchange kinetics in skeletal muscle in vivo. Magnetic Resonance in Medicine. 1999; 42(3):467–478. [PubMed: 10467291]
17. Quirk JD, Bretthorst GL, Duong TQ, Snyder AZ, Springer CS Jr. Ackerman JJ, Neil JJ. Equilibrium water exchange between the intra- and extracellular spaces of mammalian brain. Magnetic Resonance in Medicine. 2003; 50(3):493–499. [PubMed: 12939756]
18. Li X, Rooney WD, Springer CS Jr. A unified magnetic resonance imaging pharmacokinetic theory: intravascular and extracellular contrast reagents. Magnetic Resonance in Medicine. 2005; 54(6): 1351–1359. [PubMed: 16247739]
19. Bloch F. Nuclear Induction. Phys Rev. 1946; 70:460–473.
20. McConnell HM. Reaction rates by nuclear magnetic resonance. J Chem Phys. 1958; 28(3):430–431.
21. Spencer RG, Fishbein KW. Measurement of spin-lattice relaxation times and concentrations in systems with chemical exchange using the one-pulse sequence: breakdown of the Ernst model for partial saturation in nuclear magnetic resonance spectroscopy. J Magn Reson. 2000; 142(1):120–135. [PubMed: 10617442]
22. Bogdanov AA Jr. Weissleder R, Frank HW, Bogdanova AV, Nossif N, Schaffer BK, Tsai E, Papisov MI, Brady TJ. A new macromolecule as a contrast agent for MR angiography: preparation, properties, and animal studies. Radiology. 1993; 187(3):701–706. [PubMed: 8497616]
23. Franklin, KBJPG. The Mouse Brain in Stereotaxic Coordinates:. Academic Press; 2007.
24. Gumerlock MK, Belshe BD, Madsen R, Watts C. Osmotic blood-brain barrier disruption and chemotherapy in the treatment of high grade malignant glioma: patient series and literature review. J Neurooncol. 1992; 12(1):33–46. [PubMed: 1541977]
25. Fortin D, Gendron C, Boudrias M, Garant MP. Enhanced chemotherapy delivery by intraarterial infusion and blood-brain barrier disruption in the treatment of cerebral metastasis. Cancer. 2007; 109(4):751–760. [PubMed: 17211866]
26. Rapoport SI. Osmotic opening of the blood-brain barrier: principles, mechanism, and therapeutic applications. Cellular and Molecular Neurobiology. 2000; 20(2):217–230. [PubMed: 10696511]
27. Ravussin P, Archer DP, Tyler JL, Meyer E, Abou-Madi M, Diksic M, Yamamoto L, Trop D. Effects of rapid mannitol infusion on cerebral blood volume. A positron emission tomographic study in dogs and man. J Neurosurg. 1986; 64(1):104–113. [PubMed: 3079823]
28. Lin W, Paczynski RP, Kuppusamy K, Hsu CY, Haacke EM. Quantitative measurements of regional cerebral blood volume using MRI in rats: effects of arterial carbon dioxide tension and mannitol. Magnetic Resonance in Medicine. 1997; 38(3):420–428. [PubMed: 9339444]
29. Reivich M. Arterial Pco2 and Cerebral Hemodynamics. The American journal of physiology. 1964; 206:25–35. [PubMed: 14117646]
30. Belliveau JW, Rosen BR, Kantor HL, Rzedzian RR, Kennedy DN, McKinstry RC, Vevea JM, Cohen MS, Pykett IL, Brady TJ. Functional cerebral imaging by susceptibility-contrast NMR. Magn Reson Med. 1990; 14(3):538–546. [PubMed: 2355835]
31. Clemedson CJ, Hartelius H, Holmberg G. The influence of carbon dioxide inhalation on the cerebral vascular permeability to trypan blue (the blood-brain barrier). Acta Pathol Microbiol Scand. 1958; 42(2):137–149. [PubMed: 13508256]
32. Cutler RW, Barlow CF. The effect of hypercapnia on brain permeability to protein. Arch Neurol. 1966; 14(1):54–63. [PubMed: 5900231]
33. Pakulski C. The influence of acute hypercapnia on the permeability of the blood-brain barrier for gentamycin under conditions of general anesthesia in rabbits. Annales Academiae Medicae Stetinensis. 1998; 44:285–296. [PubMed: 9857545]
34. Johansson B, Nilsson B. The pathophysiology of the blood-brain barrier dysfunction induced by severe hypercapnia and by epileptic brain activity. Acta Neuropathologica. 1977; 38(2):153–158. [PubMed: 878851]

35. Hirt L, Ternon B, Price M, Mastour N, Brunet JF, Badaut J. Protective role of early Aquaporin 4 induction against postischemic edema formation. J Cereb Blood Flow Metab. 2009; 29(2):423–433. [PubMed: 18985050]

36. Rapoport SI, Fredericks WR, Ohno K, Pettigrew KD. Quantitative aspects of reversible osmotic opening of the blood-brain barrier. Am J Physiol. 1980; 238(5):R421–431. [PubMed: 7377381]

37. Packard SD, Mandeville JB, Ichikawa T, Ikeda K, Terada K, Niloff S, Chiocca EA, Rosen BR, Marota JJ. Functional response of tumor vasculature to PaCO2: determination of total and microvascular blood volume by MRI. Neoplasia. 2003; 5(4):330–338. [PubMed: 14511404]

38. Kim, Y.; Jennings, D.; Benner, T.; Kwon, S.; Cho, G.; Kim, J.; Farrar, C.; Caravan, P.; Rosen, B.; Sorensen, A. Detection of abnormal water exchange rate in brain tumor patients. Montreal, Quebec, Canada; 2011.

39. Ribeiro Mde C, Hirt L, Bogousslavsky J, Regli L, Badaut J. Time course of aquaporin expression after transient focal cerebral ischemia in mice. J Neurosci Res. 2006; 83(7):1231–1240. [PubMed: 16511868]

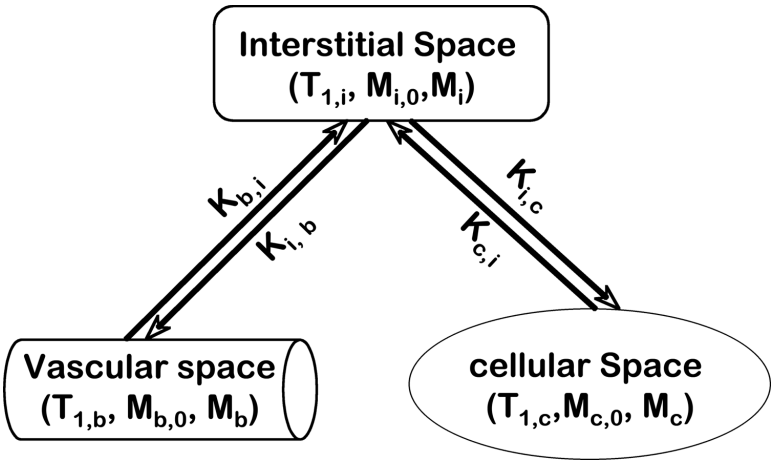

Figure 1.

A three-compartment tissue model consisting of vascular, cellular, and extravascular-extracellular (interstitial) spaces, with no direct water exchange between intravascular and intracellular spaces.

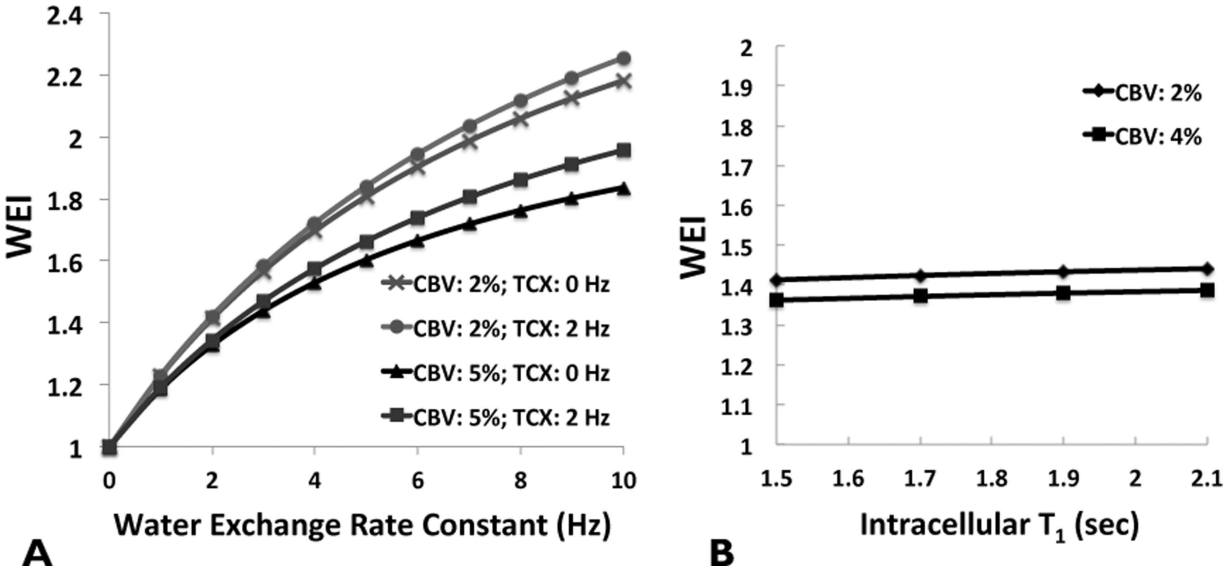

Figure 2.

(A) Computer simulations showing the effect of the intravascular blood volume and transcytolemmal water exchange on the linearity of the relationship between the WEI (water exchange index) and the WER (transvascular water exchange rate). (B) Computer simulations demonstrating the effect of intracellular T_1 on the WEI measurement. An increase in the CBV leads to a decrease in the linearity of the WEI-WER relation. This decreased linearity for high WER translates into a decreased sensitivity of the WEI to changes in the WER. The inclusion of transcytolemmal water exchange helps to slightly extend the linear regime to higher WER. Changes in the intracellular T_1 have negligible effect on the WEI measurement.

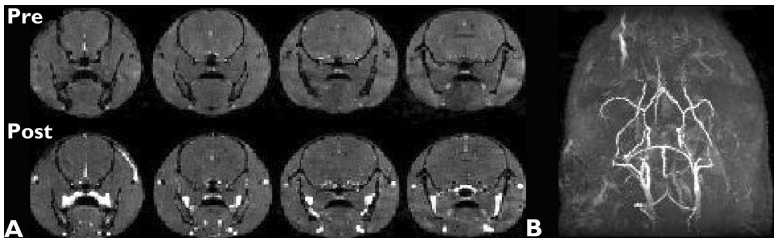

Figure 3.
(A) Representative T1-weighted gradient-echo images of a mouse brain acquired pre and post Gd-PGC injection; (B) MRI angiography of the same mouse (without contrast agent).

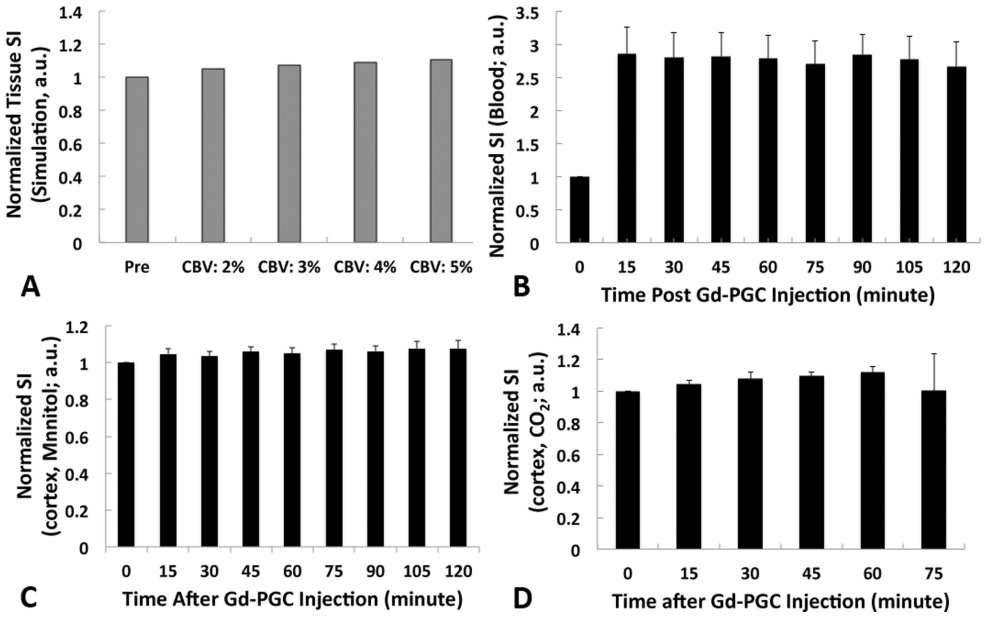

Figure 4.

(A) Simulation of the tissue signal intensity performed for blood volumes ranging from 2–5% observed only a slight increase in signal intensity following contrast agent administration due to the increased signal from vascular water. (B) The near constant signal intensity measured over a two-hour time period for blood, following contrast agent injection, indicates that Gd-PGC has a very long blood half-life. (C) Experimental measurements of cortex tissue signal intensity for both Mannitol and (D) CO_2 challenges observe a similar slight increase indicating that Gd-PGC does not extravasate into the tissue.

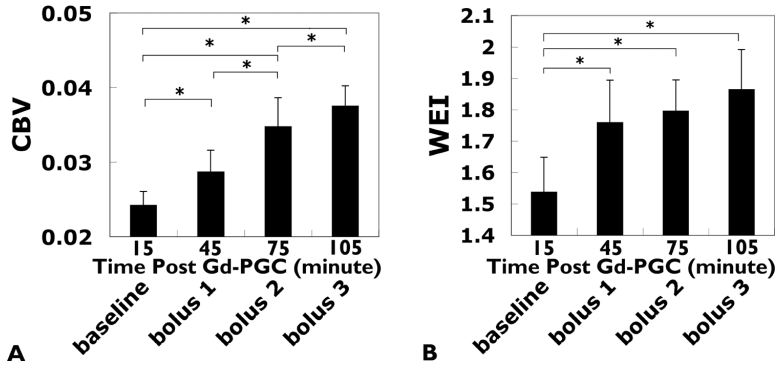

Figure 5.

Changes in the CBV (A) and WEI (B) of cortex brain tissue in response to Mannitol administration. While the CBV continued to increase after each Mannitol bolus injection, the WEI increased significantly only after the first bolus injection. Subsequent Mannitol injections had no significant effect on the WEI.

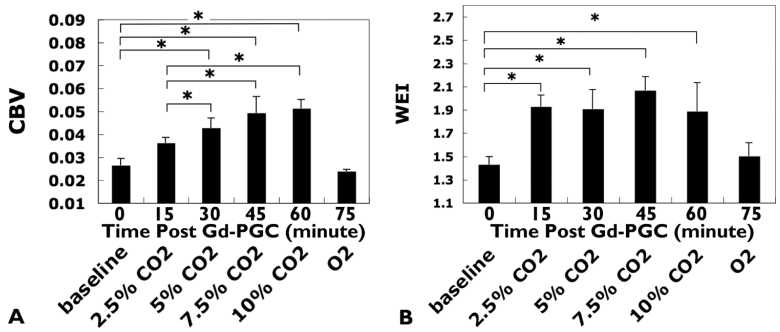

Figure 6.

Change in the CBV (A) and WEI (B) during graded CO_2 challenge. The CBV showed a linear relationship with the amount of CO_2 in the breathing gas mixture and became saturated when the amount of CO_2 in the gas mixture reached 10%. In contrast, the WEI increased significantly only after 2.5% CO_2 inhalation, and was not affected by further increases of CO_2 in the gas mixture. Both the CBV and the WEI showed strong response to 100% O_2.

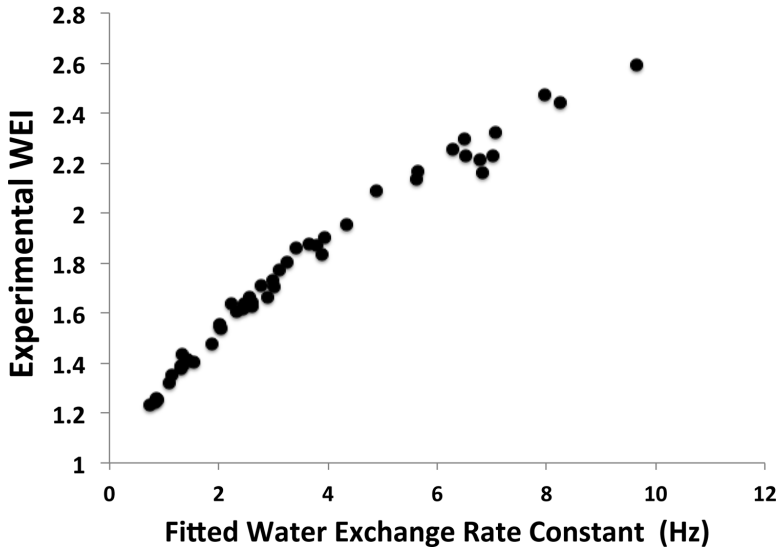

Figure 7.

Scatter plot of the experimentally determined WEI as a function of the calculated WER. The WERs were calculated from fitting the flip-angle dependence of the MRI signal using the two-compartment model and the imaging parameters (TR and flip angles) and experimentally measured T1's and CBV. The WEI is a highly linear function of the WER over the 1–5Hz WER range.